SC/F16/JR/36

Effects of persistent organochlorine exposure on the liver transcriptome of the common minke whale (Balaenoptera acutorostrata) from the North Pacic

Satoko Niimi, Mai Imoto, Tatsuya Kunisue, Michio X. Watanabe, Eun-Young Kim, Kei Nakayama, Genta Yasunaga, Yoshihiro Fujise, Shinsuke Tanabe and Hisato Iwata

INTERNATIONAL WHALING COMMISSION

Ecotoxicology and Environmental Safety 108 (2014) 95–105

Contents lists available at ScienceDirect

Ecotoxicology and Environmental Safety

journal homepage: www.elsevier.com/locate/ecoenv

Effects of persistent organochlorine exposure on the liver transcriptome of the common minke whale (*Balaenoptera acutorostrata*) from the North Pacific

Satoko Niimi [a], Mai Imoto [a], Tatsuya Kunisue [a], Michio X. Watanabe [a], Eun-Young Kim [b], Kei Nakayama [a], Genta Yasunaga [c], Yoshihiro Fujise [c], Shinsuke Tanabe [a], Hisato Iwata [a,*]

[a] Center for Marine Environmental Studies (CMES), Ehime University, Bunkyo-cho 2-5, Matsuyama 790-8577, Japan
[b] Department of Life and Nanopharmaceutical Science and Department of Biology, Kyung Hee University, Hoegi-Dong, Dongdaemun-Gu, Seoul 130-701, Republic of Korea
[c] The Institute of Cetacean Research, Toyomi-cho 4-5, Chuo-ku, Tokyo 104-0055, Japan

ARTICLE INFO

Article history:
Received 18 March 2014
Received in revised form
20 June 2014
Accepted 20 June 2014

Keywords:
Minke whale
Transcriptome
Organochlorines
Dioxins
Kynureninase

ABSTRACT

Hepatic concentrations of persistent organochlorines (OCs) were determined in the common minke whale (*Balaenoptera acutorostrata*) from the North Pacific. To investigate the effects of OCs on the transcriptome in the minke whale, the present study constructed a hepatic oligo array of this species where 985 unique oligonucleotides were spotted and further analyzed the relationship between the OC levels and gene expression profiles of liver tissues. The stepwise multiple linear regression analysis identified 32 genes that correlated with hepatic OC levels. The mRNA expression levels of seven cytochrome P450 (CYP) genes, *CYP1A1*, *1A2*, *2C78*, *2E1*, *3A72*, *4A35*, and *4V6* showed no clear correlations with the concentration of each OC, suggesting that the accumulated OCs in the liver did not reach levels that could alter CYP expression. Among the genes screened by the custom oligo array analysis, hepatic mRNA expression levels of 16 genes were further measured using quantitative real-time reverse transcription polymerase chain reaction. The mRNA levels of vitamin D-binding protein (DBP) were negatively correlated with non-*ortho* coplanar polychlorinated biphenyl (PCB) levels. Androgen receptor-associated coregulator 70 (ARA70) expression levels showed a significant positive correlation with concentrations of non-*ortho* coplanar PCB169. These correlations suggest that coplanar PCB-reduced DBP expression could suppress vitamin D receptor-mediated signaling cascades in peripheral tissues. Alternatively, the suppression of vitamin D receptor signaling cascade could be enhanced through competition with the androgen receptor signaling pathway for ARA70. In addition, a negative correlation between kynureninase and PCB169 levels was also observed, which suggest an enhanced accumulation of an endogenous aryl hydrocarbon receptor agonist, kynurenine in the minke whale population. Further studies are necessary to translate the changes in the transcriptome to toxicological outcomes including the disruption of the nervous and immune systems.

1. Introduction

Persistent organochlorine compounds (OCs) such as polychlorinated biphenyls (PCBs), 1,1,1-trichloro-2,2-bis(*p*-chlorophenyl) ethane (DDT), and its metabolite, DDE, have been detected in a variety of environmental media (Iwata et al., 1993). Due to their high bioaccumulation and toxic potentials, the contamination of OCs in wildlife has been of great concern (Tanabe et al., 1994).

The levels of OCs in wild animal populations have been well documented; however, the information on its effects remains insufficient, especially at the molecular level. Regulatory programs in developed countries have started to incorporate tests and endpoints that capture the effects of chemicals on specific signaling pathways in animals (Ankley et al., 2010). Hence, 21st century ecological testing and screening programs for chemicals should be highly comprehensive and promptly implemented (Villeneuve and Garcia-Reyero, 2011). On the other hand, the majority of the methods used for ecological testing virtually relies on whole animal exposures that focus on its effects on survival, growth, and reproduction. These types of tests are resource-oriented and time-intensive; this makes it technically difficult to address wild species, particularly large-sized animals.

Animals react to chemical exposures by changing the expression patterns of their transcriptome (Van Aggelen et al., 2010;

* Corresponding author.
E-mail address: iwatah@agr.ehime-u.ac.jp (H. Iwata).

http://dx.doi.org/10.1016/j.ecoenv.2014.06.028
0147-6513/

Williams et al., 2003; Hirakawa et al., 2011). Thus, comprehensive monitoring of the transcriptome in animals of concern, also known as transcriptomics, will identify the critical targets of chemicals and reveal new mechanisms of action. For gene expression analysis, particularly at the transcriptome level, the use of the microarray technique has recently been recognized as the standard methodology and continues to improve in terms of efficiency, data enrichment, and cost (Van Aggelen et al., 2010). In toxicological studies, the microarray has been frequently used to comprehensively determine changes in gene expression profiles in organisms exposed to not only drugs and pharmaceuticals but also environmental contaminants. Hence, this technique could play an important role in screening chemicals and in assessing the health of animals. Molecular responses of murine models to OC exposure have been detected using microarrays (Zeytun et al., 2002; Boverhof et al., 2005, 2006; Vezina et al., 2004; Adeeko et al., 2003; Kopec et al., 2010). Such studies have identified genes responsive to OCs, as well as evaluated potential effects by associating histopathological features with specific gene expression profiles. These observations have thus facilitated the implementation of transcriptomics as a diagnostic tool in ecotoxicology (Van Aggelen et al., 2010). However, most ecotoxicology studies have used murine mammals that have been propagated in the laboratory and may thus inaccurately represent the gene expression profiles of wild animals that are subjected to chronic and/or long-term exposure to chemicals (Williams et al., 2003; Nakayama et al., 2006; Hirakawa et al., 2011), while inbred murine animals can diminish their genetic diversity which may contribute to significant differences in responses to chemical exposure. Comprehensive monitoring of changes in gene expression in wild species may lead to the development of molecular markers that aid in identifying causative chemicals and toxic mechanisms of action.

Our previous studies have revealed that common minke whales (*Balaenoptera acutorostrata*) from the North Pacific accumulate classical OCs including PCBs (sum of congeners), DDTs (*p,p′*-DDT, *p,p′*-DDD, and *p,p′*-DDE), hexachlorocyclohexanes (HCHs; α-, β-, and γ-HCH), chlordanes (CHLs; *cis*-chlordane, *trans*-chlordane, *cis*-nonachlor, *trans*-nonachlor, and oxychlordane) and hexachlorobenzene (HCB) in the liver and blubber (Aono et al., 1997; Niimi et al., 2005). Furthermore, by using a cDNA library generated from minke whale livers, we have identified seven cytochrome P450 (CYP) isozymes, including *CYP1A1* (Accession no. AB231891), *CYP1A2* (AB231892), *CYP2C78* (AB290008), *CYP2E1* (AB290010), *CYP3A72* (AB290009), *CYP4A35* (AB290011), and *CYP4V6* (AB290012) that might potentially respond to environmental contaminants such as OCs at the transcriptional level and be involved in their metabolism. We then determined their full-length cDNA sequences and hepatic mRNA expression levels (Kim et al., 2004; Niimi et al., 2005, 2007). In addition, we carried out correlation analyses between concentrations of each OC and mRNA expression levels of each *CYP* isozyme in the liver of the minke whale population from the North Pacific. The results showed no significant correlations between the *CYP* isozyme expression levels and the OC concentrations, which indicate that these CYP enzymes were not induced by OC exposure (Niimi et al., 2007). However, the effects of OCs on the hepatic expression of genes other than these *CYPs* in the common minke whales still remain unclear. Sequence data from the whale cDNA library could be potentially employed as a diagnostic tool such as microarray for evaluating chronic exposure of complex mixtures of OCs in the whale species because it could help to establish sensitive markers that identify pathways to adverse outcomes before they are manifested in the population.

In the present study, we constructed an oligo array of the common minke whale using sequence data from the hepatic cDNA library (Niimi et al., 2007) to investigate alterations in the expression of genes other than *CYPs* that may be associated with OC accumulation in the body. In addition to chemical analyses of PCBs, DDTs, HCHs, chlordanes, and HCB that have been so far reported (Niimi et al., 2005), we further analyzed dioxins and related compounds (DRCs), including polychlorinated dibenzo-*p*-dioxins (PCDDs) and dibenzofurans (PCDFs) and coplanar (dioxin-like) PCBs as aryl hydrocarbon receptor (AHR) agonists in the liver of minke whales. Statistical analyses of correlations between hepatic OC concentrations and gene expression levels on the custom oligo array were then executed. Based on the correlation analyses, we assessed the potential effects of OCs in the whale liver.

2. Materials and methods

2.1. Samples

Liver samples of the common minke whale employed in the present study were the same as those used in our previous studies (Niimi et al., 2005, 2007). In brief, nineteen male common minke whales (nine immature and ten mature) were collected from an area of the western North Pacific (35–45°N, 140–150°E) by JARPN II (Japanese Whale Research Program under Special Permit in the Western North Pacific-Phase II) in 2001. Livers of common minke whales were immediately removed on board the research vessel after capture. Only male liver samples were used to rule out the effect of sex on gene expression profiles. The livers wrapped with aluminum foil were frozen in liquid nitrogen and subsequently stored at −80 °C in the laboratory of Ehime University until total RNA preparation. The subsamples of the livers were stored at −20 °C until DRC analysis.

2.2. Construction of custom microarray

Hepatic cDNA library of the common minke whale was prepared for the construction of an oligo array (Niimi et al., 2005). A total of 6930 clones randomly selected from the library were screened, and 1991 cDNA clones with high sequence identities with genes deposited in GenBank were obtained. Unique 70-mer oligonucleotides for 985 genes were designed and spotted in duplicate onto a TaKaRa-Hubble slide glass (Takara Bio, Inc.). Spotted genes on the oligo array were categorized according to the gene annotation presented in Table 1.

Table 1
List of genes spotted onto our custom minke whale oligo array.

Gene species	*n*
Oncogene	6
Transcriptional factor	19
Translation initiation factor	12
Elongation factor	8
Receptor	45
Transporter	23
Immune system	15
Synthetase	42
Kinase	43
Phosphatase	19
Xenobiotic metabolizing enzyme	29
Antioxidant enzyme	4
Other enzymes	288
Homeobox	1
Growth factor	7
Heat shock protein	6
Ribosomal protein	13
Glycoprotein	14
KIAA	31
RIKEN	33
MGC	50
ATP-related protein	18
Haptoglobin	2
Selenoprotein	2
Cathepsin	5
Others	250
Total	985

2.3. Oligo array analysis

Total RNAs from nineteen liver samples were individually extracted using TRIzol® reagent (Invitrogen), and the quality of each RNA sample was checked by denaturing agarose gel electrophoresis. RNA samples from three specimens that contained relatively low OC levels were pooled for use as a common reference for the following analysis. The preparation of antisense RNA (aRNA) probe, hybridization, washing, and scanning for oligo array analyses were performed according to the method of Nakayama et al. (2006) and Hirakawa et al. (2011). For the preparation of RNA probes, amino allyl antisense aRNA was amplified using 5 μg of total RNA with an Amino Allyl MessageAmp aRNA kit (Ambion), and 5 μg of aRNA was labeled with either Cy3 (data) or Cy5 (reference) (Amersham Biosciences). Excess amounts of the Cy dye were then removed using a QIAquick PCR purification kit (Qiagen K.K.). Cy3- and Cy5-labeled aRNAs were mixed and fragmented with a 5 × fragmentation buffer [0.5 M of potassium acetate, 0.15 M of magnesium acetate in 0.2 M Trisacetate (pH 8.1)]. Labeled aRNA was purified and concentrated using Microcon YM-10 filters (Millipore) for subsequent hybridization. For hybridization, a Cy dye-labeled aRNA solution was prepared using 6 × SSC, 0.2 percent SDS, 5 × Denhardt's solution (Eppendorf), and 0.1 mg/mL human Cot-I DNA® (Invitrogen). The aRNA solution was heated at 95 °C for 2 min to denature aRNA, cooled on ice, and then incubated at 65 °C for 5 min. After incubation, the aRNA solution was placed on a glass slide, and the aRNA probes were hybridized with oligonucleotides spotted on the glass slide at 65 °C for 17 h. Following hybridization, the slides were washed twice with 0.2 percent SDS in 2 × SSC at 55 °C and once with 0.2 percent SDS in 2 × SSC at 65 °C, rinsed twice with 0.2 × SSC at room temperature, and then dried by centrifugation at 800 rpm for 3 min. The washed slides were then scanned using a fluor-image analyzer (FLA-8000, Fuji Photo Film Co., Ltd.) at a wavelength of 532 nm for Cy3 and at 635 nm for Cy5.

Fluorescence intensities derived from the Cy dye-labeled aRNA probes were quantified by Array Gauge Ver 2.0 (Fuji Photo Film Co., Ltd.) in triplicate for each sample. The intensity on the surrounding area of each spot was used as a background signal. The fluorescence intensity of each spot was corrected using the background signal intensity. Expression levels of each gene were represented as data (Cy3)/reference (Cy5) ratios. The ratios were normalized using the Locfit (LOWESS) function in TIGR MIDAS (version 2.19). Data showing less than twenty percent of inter-slide variation in the gene expression levels in triplicate were subjected to the following correlation analyses with OC levels.

2.4. Quantitative assessment of array-screened gene mRNAs by real-time RT-PCR

Total RNA extracted from each liver sample was treated with DNase prior to mRNA quantification to avoid DNA contamination. The mRNA expression levels of genes, which have been associated with hepatic residue levels of OCs through an initial screening using oligo array analysis, were further measured by quantitative real-time RT-PCR. An ABI PRISM 7700 Sequence Detection System (Applied Biosystems) was utilized for real-time PCR with a TaqMan One-Step RT-PCR Master Mix Reagent Kit (Applied Biosystems). A set of specific primers and probe for each gene of interest was designed using the cDNA sequence and the Primer Express™ ver. 1.05 software program (Applied Biosystems). The final concentrations of the primers and probes in the reaction mixture and annealing temperature for real-time RT-PCR are summarized in Table 2. FAM was used as a reporter dye at the 5′-end of the probe and TAMRA was used as a quencher dye at the 3′-end. Each reaction mixture contained 50 ng or 100 ng of total RNA as template. Conditions for real-time RT-PCR were as follows: 30 min at 48 °C, 10 min at 95 °C, and 40 cycles of 15 s at 95 °C and 1 min at the corresponding annealing temperature for each set of primers (Table 2). The primers and a VIC-labeled probe for the endogenous control ribosomal RNA (rRNA) were purchased from PE Applied Biosystems. Quantitative values were obtained from the threshold PCR cycle number (Ct) at which the increase in signals associated with an exponential growth of PCR products was detected. The standard curve of PCR products was obtained using a serially diluted total RNA solution. The relative mRNA level of each sample was normalized to its rRNA content and was expressed as the ratio relative to the highest expression level among the analyzed samples.

2.5. Chemical analysis of DRCs

DRCs, including PCDD/Fs and coplanar PCBs, were analyzed following the method described by Iwata et al. (2004). Ten to twenty grams of liver samples were extracted in a Soxhlet apparatus for more than 8 h with dichloromethane (DCM). The extract was concentrated, and an aliquot was used for lipid determination. $^{13}C_{12}$-labeled PCDD/Fs and coplanar PCBs (2,3,7,8-T_4CDD/F, 1,2,3,7,8-P_5CDD/F, 1,2,3,6,7,8-H_6CDD/F, 1,2,3,7,8,9-H_6CDF, 1,2,3,4,6,7,8-H_7CDD/F, O_8CDD/F, PCB-77, -81, -118, -126, -156, -167, -169, and -189) were spiked into the remaining extract as a mixture of internal standards. Lipid and biogenic materials in this solution were removed by a gel permeation chromatography using a Bio-Bead S-X 3 packed glass column (50 cm × 2 cm i.d., Bio-Rad Laboratories). A mixture of 50 percent hexane in DCM was used as mobile phase, at a flow rate of 5 mL/min. The first 120 mL of eluted solvent was discarded, and the following 100-mL fraction, which contained PCDD/Fs and coplanar PCBs, was collected, concentrated, and passed through a 3.0-g activated silica gel-packed glass column (Wako-gel S-1, Wako Pure Chemical Industries Ltd.). PCDD/Fs and coplanar PCBs were eluted with 220 mL of hexane. After the concentration of eluate, the extract was spiked into a 10-g activated alumina-packed glass column (aluminum oxide 90, Brockman activity I, 70–230 mesh, Merck). The first fraction eluted with hexane contained most of the PCB isomers, including a large portion of mono-*ortho* coplanar congeners, and the second fraction eluted with 50 percent of DCM in hexane contained the remaining mono-*ortho* coplanar PCBs, non-*ortho* coplanar PCBs, and PCDD/Fs. The second fraction eluted from the activated alumina column was treated with a 1.0-g activated carbon-dispersed silica gel-packed glass column (1 cm i.d., Kanto Chemical Co. Inc.). The first fraction was collected with 25 percent of DCM in hexane for mono-*ortho* coplanar PCBs and combined with the first fraction obtained from the alumina column. The second fraction eluted with 220 mL of toluene contained non-*ortho* coplanar PCBs and PCDD/Fs. Both fractions were concentrated to near dryness, and $^{13}C_{12}$-labeled CB-105, CB-157, and CB-180 prepared in decane were added to the combined first fraction, and $^{13}C_{12}$-labeled 1,2,3,4-T_4CDD and 1,2,3,7,8,9-H_6CDD to the second fraction. The identification and quantification of mono-*ortho* coplanar PCBs were performed using a gas chromatograph (GC) (Agilent 6890 series, Agilent Technology) with a benchtop double-focusing mass selective detector (MSD) (JEOL GC-MateII, JEOL Ltd.). The GC column used was a DB-1 fused silica capillary (60 m length, 0.25 mm i.d., 0.25-μm film thickness, J&W Scientific, Inc.). The identification and quantification of non-*ortho* coplanar PCBs and PCDD/Fs were performed using a GC (Agilent 6890 series) with a high-resolution MSD (JEOL JMS-700D). Chromatographic separation was accomplished by using a DB5ms fused silica capillary column (60 m length, 0.25 mm i.d., 0.1-μm film thickness, Varian, Inc.). The first and second highest ions were monitored for the identification of individual congeners, except for P_5CDD at ions of $[M]^+$ and $[M^{+2}]^+$.

All the congeners were quantified using an isotope dilution method for the corresponding $^{13}C_{12}$-congeners when the isotope ratio was within fifteen percent of the theoretical ratio and the peak area was more than five times the noise or procedure blank level. Recoveries for the $^{13}C_{12}$-labeled PCDD/Fs and coplanar PCBs, which were added prior to gel permeation chromatography, were within 60–120 percent. The 2,3,7,8-T_4CDD toxic equivalents (TEQs) were calculated using toxic equivalency factors determined for mammalian species (Van den Berg et al., 2006).

2.6. Statistical analyses

The Mann–Whitney U test was employed to detect differences in DRC concentrations between immature and mature animals. Correlations among OC concentrations were analyzed by using Pearson's correlation test. Correlations of concentrations of a single or mixture of OCs with mRNA expression levels were examined by using stepwise multiple linear regression analyses. Correlations of the microarray data with the real-time RT-PCR data for each gene, and the relationships between mRNA expression levels measured by the real-time RT-PCR and OC concentrations were analyzed by using Spearman's rank correlation test. All statistical analyses were performed using StatView 5 (SAS Institute Inc., Cary, NC) and SPSS 12.0J (SPSS, Tokyo, Japan). A p value of < 0.05 was regarded as statistically significant.

3. Results

3.1. Concentrations of DRCs in the liver of the common minke whale

DRCs were detected in all liver samples of the common minke whales analyzed in this study (Table 3). Hepatic residue levels of other OCs in this population have been previously reported in detail (Niimi et al., 2005). While only a few PCDD/F congeners (O_8CDD, 2,3,7,8-T_4CDF, 2,3,4,7,8-P_5CDF, and 2,3,4,6,7,8-H_6CDF) were detected at trace levels (< 0.01–0.70 pg/g wet wt), the concentrations of total coplanar PCBs were relatively high (690–8900 pg/g wet wt). The residue levels of non-*ortho* coplanar PCB169 and mono-*ortho* coplanar PCBs, except for PCB105, 114, and 123, in mature male whales were significantly higher than those in immature male whales ($p < 0.05$). Hepatic total TEQ levels were within the range of 0.54–3.2 pg TEQ/g wet wt. The contribution of TEQs derived from non-*ortho* coplanar PCBs to total TEQs was the most dominant (Table 3).

Significant positive correlations among residue levels of OCs were detected in all the analyzed samples (Table 4). The inter-correlations of OC levels indicated concurrent exposure of this North Pacific whale population. This is probably due to similarities

Table 2
List of primer pairs and probes designed for the quantification of the mRNA expression levels of genes by real-time RT-PCR.

Gene name	Primer and probe sequences 5′ to 3′		Amplicon (bp)	Primer and probe concentration (nM)	Anealing temperature (°C)	Total RNA as template (ng)
CYP1A1	F	CCGTATCCGGGACATCACAG	104	300	53	50
	R	CGACATTAACGATCTTCTCATCTGA		300		
	Probe	CTGTCAGGGCAAGAGACTGGACGAGAA		250		
CYP1A2	F	GGTGCCCTGTTCAAGCACTACGA	126	900	57	100
	R	AGATGGCTGTTGTGATTGGATCAAAC		900		
	Probe	CAACCTTGTCAACGACATCTTCGCAGCC		250		
CYP2C78	F	AGTTTCTGGTGGAGGAGCTCAGGA	103	900	56	100
	R	GTTGAAGAGGATGGAGCAGATCACA		900		
	Probe	TTCACCCTCTCCTGTGCTTCCTGCAA		250		
CYP2E1	F	CTACAACGTCATCTCCGACATCCTC	108	900	55	100
	R	GCTACTGAGCAGGTAGAAGTTCTCATTG		900		
	Probe	CGACTACAATGACAAGACGGCTCTG		250		
CYP3A72	F	GCTGGCTACGAGACCACTAGCAAT	102	900	54	100
	R	AAGTTGCATCAATCTCCTCCTGC		900		
	Probe	AATTGGCCACTCACCCTGATGTCCAG		250		
CYP4A35	F	GGAGCAGCTTGTCTGACGTGGA	112	900	57	100
	R	GTGGGAGGCCAGAGCATAGAGGAT		900		
	Probe	CCGAAGTGGATACGTTCATGTTCGAGGGTC		250		
CYP4V6	F	CCTATGCACTGCACAGAGATCAAAGG	105	900	57	100
	R	ACATATGCGTATGAATGACGTCCTTTC		900		
	Probe	CCTGAGGAATTCAAGCCAGAACGGTTCTT		250		
2',5'-Oligoadenylate synthetase (OAS1)	F	AGTGCGTGGAGTTTGATGTCCT	101	900	53	50
	R	CTCTCGGATAAGCTGGACGTAGA		900		
	Probe	TTGACCAGAGGCTACAGACCTGACCCTAAA		250		
ATP synthase gamma subunit precursor (ATP5C1)	F	GGCTGATATTAAGGTGCCTGAAGA	91	900	53	50
	R	CGAGGAATGAATAGCACCACAA		900		
	Probe	ACATCTCCTTATTGGTGTGTCCTCAGACCG		250		
Solute carrier family 27, member 5 (SLC27A5)	F	GCATGGTGTGACTGTGATCCA	101	900	57	50
	R	TTGCCAGGCGGACTTTATGT		900		
	Probe	TCCTGCGGTACCTGTGCAACACTCC		250		
Acetyl-CoA C-acetyltransferase (ACAT1)	F	GAACACCCATTGGATCCTTTCTA	101	900	57	50
	R	TGGAATCCCTGCCTTTTCAA		900		
	Probe	CTTTCCTCTCTGCCAGCCACTAAACTTGGTT		250		
Histamine N-metyltransferase (HNMT)	F	TTGGTTTCTGACCACAGCAGAT	101	900	57	50
	R	GGCAGCTTCTCGTCCATGA		900		
	Probe	TTGAATCTTTCCGGAGGTTTCTCGACAATTC		250		
Urate oxidase precursor (UOX)	F	GTGCAACTTACTCTGAGCTCCAAA	101	900	58	100
	R	TTTGCCAGGACATGAACTGTGT		900		
	Probe	TTCAGACCTCATCCCTACAGACACCATCAA		250		
Lactate dehydrogenase A (LDHA)	F	TCCAACATGGCAGCCTTTTC	101	900	58	100
	R	TGCTCCAGCTGTGATAATAACCA		900		
	Probe	TTAAAACACCAAAAATCGTCTCTGGCAAAGACT		250		
Paraoxonase 2 (PON2)	F	ACCTTCCAAACTGCCACCTG	91	300	59	100
	R	CCCACACTAAAGAAGGCCGAC		300		
	Probe	CGAAGCTGGCTCTGAAGATATTGACATACTTCC		250		
Caspase 6 (CASP6)	F	GCTCACGGTGCAGGTGAAC	81	900	59	50
	R	GTACGTTTCTGCCGGATCAAA		900		
	Probe	CATGACAGAAACAGATGCCTTCCCTATGAGA		250		
Cysteine dioxygenase 1 (CDO1)	F	AGGACATGGCAGCAGTATCCA	91	300	58	50
	R	CCAGGCAAATAACGTCTCCTTT		300		
	Probe	ATCACACTGACTCCCACTGCTTTCTGAAGATG		250		
Androgen receptor-associated protein 70 (ARA70)	F	GCACCACATCTGTCCCTCTCA	101	900	58	50
	R	GAGCCAGTCCTGCAGATTGG		900		
	Probe	CAGCGGTCGCCAGGCTCCTTACATAC		250		
Vitamin D binding protein (DBP)	F	CCACTCTGGGAATGACATCTGA	101	300	58	50
	R	GAGGCTCTTGCAGCTGATAACA		300		
	Probe	AGCCTAACCCAAGCAAAACCAGAGTTCCT		250		
Kynureninase (KYNU)	F	GTCCGACGCATCGCATCT	91	900	58	50
	R	TGAAGTGCCTCAGCTTATCTTCCT		900		
	Probe	AACAGATGAGAGAGTTGCCCTCCGCC		250		
S3 ribosomal protein (RPS3)	F	AATCCATGAAGTTCGTGGATGG	101	900	58	50
	R	CACACCCTGTCTGAGCAGCA		900		
	Probe	TAACTACTATGTTGATACTGCCGTGCGCCA		250		

Table 2 (*continued*)

Gene name	Primer and probe sequences 5′ to 3′		Amplicon (bp)	Primer and probe concentration (nM)	Anealing temperature (°C)	Total RNA as template (ng)
Ribosomal protein L13a (RPL13a)	F	GATCCCGCCACCCTATGAC	91	300	58	50
	R	GTAGGCAAACTTCCGTGTAGGCT		300		
	Probe	ATGGTGGTTCCTGCCGCCCTC		250		
Acidic ribosomal phosphoprotein P0 (RPLP0)	F	ACAGTGCCTGCCCAGAACAC	91	300	58	50
	R	TGGTGCCCCTGGAGATTTTAG		300		
	Probe	AGACCTCCTTCTTCCAGGCTTTAGGCATCA		250		

F: forward primer.
R: reverse primer.

in sources, physicochemical characteristics, and/or toxicokinetics among these environmental pollutants. Based on the results of intercorrelation analyses of OC levels, it may be difficult to identify the causative OC compound that is responsible for the altered gene expression levels, even when the accumulation level of a single compound exhibited a significant correlation with the expression level of a certain gene. Hence, the most plausible approach is to treat all the tested OCs as potential candidates that induce changes in expression levels of a particular gene in case that a significant correlation is obtained.

3.2. Gene expression analysis

Stepwise multiple linear regression analysis using oligo array data identified 21 genes showing associations between expression patterns and TEQ levels, and twelve genes presenting relationships with other OCs in the liver of common minke whales (Tables 5 and 6). The mRNA expression levels of paraoxonase 2 were correlated with both of non-*ortho* coplanar PCB-derived TEQ and HCB levels. The total 32 genes were classified into functional categories, which include receptors, ribosomal proteins, synthetases, phosphatases, and other enzymes, as well as specific cellular activities such as apoptosis, immune function, ATP synthesis, citric acid cycle, and fatty acid metabolism.

Among the genes screened by our oligo array analysis, mRNA expression levels of 16 genes, including androgen receptor-associated coregulator 70 (*ARA*70), ATP synthase gamma chain (*ATP*5*C*1), paraoxonase 2 (*PON*2), ribosomal protein S3 (*RPS*3), ribosomal protein L13a (*RPL*13*A*), acidic ribosomal phosphoprotein P0 (*RPLP*0), kynureninase (*KYNU*), histamine *N*-methyltransferase (*HNMT*), vitamin D binding protein (*DBP*), 2′,5′-oligoadenylate synthetase 1 (*OAS*1), solute carrier family 27 (fatty acid transporter) member 5 (*SLC*27*A*5), urate oxidase precursor (*UOX*), cysteine dioxygenase type 1 (*CDO*1), acetyl-coenzyme A acetyltransferase 1 (*ACAT*1), lactate dehydrogenase A (*LDHA*), and caspase 6 (*CASP*6) were further measured using quantitative real-time RT-PCR. Significantly positive correlations in expression levels between the oligo array and real-time RT-PCR analyses were observed in seven out of the sixteen genes, which included *ARA*70, *RPS*3, *KYNU*, *HNMT*, *CDO*1, *LDHA*, and *CASP*6 (Table 7). Significant correlations were also observed between some of OC levels and *DBP*, *ARA*70, *KYNU*, *RPS*3, *OAS*1, *LDHA*, and *CASP*6 mRNA expression levels that were measured using both the oligo array and real-time RT-PCR analyses. The mRNA levels of *DBP* and *KYNU* measured by real-time RT-PCR were negatively correlated with TEQ levels from non-*ortho* coplanar PCBs, particularly with PCB126 (Fig. 1A and B). As for *ARA*70 levels quantified with real-time RT-PCR, a significant positive correlation with PCB169 levels was detected (Fig. 1C). Positive correlations were detected between the expression levels of *RPS*3, *OAS*1, *LDHA*, and *CASP*6 and γ-HCH levels (data not shown).

Although the CYP isozymes including *CYP*1*A*1, *CYP*1*A*2, *CYP*2*C*78, *CYP*2*E*1, *CYP*3*A*72, *CYP*4*A*35, and *CYP*4*V*6 were spotted onto our whale oligo array, no correlations were established between these enzymes and OC levels. Similar findings were obtained from real-time RT-PCR analysis.

4. Discussion

4.1. Levels of DRC residue

The detected levels of DRCs in the liver of minke whales from the North Pacific were in the following decreasing order: mono-*ortho* PCBs > non-*ortho* PCBs > PCDFs > PCDDs (Table 3). This accumulation pattern, particularly characterized by traceable levels of PCDDs in the whales, was apparently similar to that observed in other oceanic vertebrate species (Kunisue et al., 2006; Kubota et al., 2010). Previous investigations have reported higher concentration ratios of PCDFs/PCDDs in oceanic animals than that in animals inhabiting terrestrial and coastal areas, indicating that selective exposure to PCDFs occurs in the open seas (Kunisue et al., 2006). The high PCDFs/PCDDs ratio in oceanic animals may be attributable to higher atmospheric transport potential of PCDFs than PCDDs, which is reflected by the higher vapor pressure (P_L) and lower octanol-air partition coefficient (K_{OA}) in PCDFs than in PCDDs, and/or to the release of PCDFs as impurities from technical PCB formulations used as antifouling paints in commercial vessels (Kunisue et al., 2006). The residue levels of non-*ortho* coplanar PCB169 and mono-*ortho* coplanar PCB118, 156, 157, 167, and 189 in mature whales were significantly higher than those in immature individuals (Table 3). This observation suggests that these congeners are constantly supplied through the oceanic food web and persist in the liver of minke whales.

TEQ levels detected in the liver of minke whales were compared to those of other vertebrate species inhabiting oceanic ecosystems. Data on DRC concentrations in cetaceans were mostly derived from blubber analysis, and TEQ levels were thus based on lipid weight analysis. Hence, the minke whale wet weight-based TEQ data of this study were converted to lipid weight basis in order to compare these with the blubber data of other cetaceans (Table 3). TEQ levels of the minke whales (16–85 pg TEQ/g lipid wt) were lower than those detected in the blubber of cetaceans, which include Stejneger's beaked whale (120–230 pg TEQ/g lipid wt) and the killer whale (110–440 pg TEQ/g lipid wt) from Japanese coastal waters (Kajiwara et al., 2004, 2006). This may be attributable to differences in prey species and trophic position in the ecosystem; the prey species of the western North Pacific common minke whale population consists of pelagic zooplankton and schools of small fishes (Tamura and Fujise, 2002), whereas Stejneger's beaked whale mostly feeds on herring, mackerel, and cephalopods. The killer whale is a real apex predator in the

Table 3
Arithmetic mean and range of hepatic concentrations of dioxins and related compounds and other organochlorines in the common minke whale from the North Pacific.

	Immature		Mature		Immature		Mature	
Sample number	9		10		9		10	
Dioxins and related compounds	Concentration (pg/g wet wt)				Concentration (pg/g lipid wt)			
PCDDs								
2,3,7,8-T_4CDD	< 0.01		< 0.01		< 0.20		< 0.20	
1,2,3,7,8-P_5CDD	< 0.01		< 0.01		< 0.20		< 0.20	
1,2,3,4,7,8-H_6CDD	< 0.03		< 0.01		< 0.60		< 0.60	
1,2,3,6,7,8-H_6CDD	< 0.03		< 0.03		< 0.60		< 0.60	
1,2,3,7,8,9-H_6CDD	< 0.03		< 0.03		< 0.60		< 0.60	
1,2,3,4,6,7,8-H_7CDD	< 0.05		< 0.03		< 1.0		< 1.0	
O_8CDD	0.24	(< 0.10–0.70)	0.18	(< 0.10–0.66)	6.7	(< 2.0–21)	4.8	(< 2.0–20)
PCDFs								
2,3,7,8-T_4CDF	0.12	(< 0.01–0.48)	0.087	(< 0.10–0.19)	3.4	(< 0.20–13)	2.1	(< 0.2–4.6)
1,2,3,7,8-P_5CDF	< 0.01		< 0.01		< 0.20		< 0.20	
2,3,4,7,8-P_5CDF	0.3	(0.12–0.61)	0.25	(0.15–0.39)	8.7	(3.6–16)	6.3	(4.3–9.8)
1,2,3,4,7,8-H_6CDF	< 0.03		< 0.03		< 0.60		< 0.60	
1,2,3,6,7,8-H_6CDF	< 0.03		< 0.03		< 0.60		< 0.60	
1,2,3,7,8,9-H_6CDF	< 0.03		< 0.03		< 0.60		< 0.60	
2,3,4,6,7,8-H_6CDF	0.1	(< 0.03–0.20)	0.12	(< 0.03–0.29)	2.8	(< 0.6–5.3)	2.7	(< 0.6–6.0)
1,2,3,4,6,7,8-H_7CDF	< 0.05		< 0.05		< 1.0		< 1.0	
1,2,3,4,7,8,9-H_7CDF	< 0.05		< 0.05		< 1.0		< 1.0	
O_8CDF	< 0.10		< 0.10		< 2.0		< 2.0	
ΣPCDDs[b]	0.31	(< 0.13–0.78)	0.26	(< 0.13–0.74)	8.3	(< 2.6–23)	6.4	(< 2.6–22)
ΣPCDFs[b]	0.68	(0.33–1.4)	0.60	(0.32–0.94)	18	(8.1–36)	14	(8.0–19)
Σ PCDD/Fs	0.99	(0.50–1.8)	0.87	(0.52–1.3)	26	(12–46)	20	(13–30)
Non-*ortho* co-PCBs								
3,3′,4,4'-T_4CB (77)	1.5	(0.86–3.2)	1.3	(0.96–1.6)	44	(25–86)	33	(23–41)
3,4,4′,5-T_4CB (81)	1.5	(0.73–4.0)	1.6	(0.88–2.8)	44	(22–110)	41	(22–86)
3,3',4,4',5-P_5CB (126)	11	(4.1–27)	12	(7.0–25)	310	(120–720)	310	(190–550)
3,3',4,4',5,5′-H_6CB (169)	2.0	(0.91–4.5)	4.2	(1.3–10)	56	(27–120)	100	(37–210)
Mono-*ortho* co-PCBs								
2,3,3′,4,4'-P_5CB (105)	180	(53–430)	130	(62–300)	5100	(1700–12,000)	3100	(1900–5500)
2,3,4,4′,5-P_5CB (114)	29	(10–54)	63	(14–140)	850	(390–1500)	1500	(390–2600)
2,3′,4,4′,5-P_5CB (118)	1200	(450–2200)	3000	(500–6600)	3300	(1500–59,000)	71,000	(14,000–130,000)
2′,3,4,4',5-P_5CB (123)	16	(8.3–31)	27	(11–59)	480	(270–830)	660	(300–1200)
2,3,3′,4,4′,5-H_6CB (156)	97	(51–160)	350	(49–760)	2900	(1400–4900)	8400	(1400–16,000)
2,3,3′,4,4′,5′-H_6CB (157)	45	(23–86)	140	(27–340)	1400	(640–2700)	3300	(750–6100)
2,3′,4,4′,5,5′-H_6CB (167)	65	(33–110)	260	(30–590)	1900	(910–3400)	6300	(930–13,000)
2,3,3′,4,4′,5,5′-H_7CB (189)	22	(10–29)	54	(22–100)	680	(260–960)	1400	(510–3100)
Σnon-*ortho* co-PCBs	16	(6.6–38)	20	(11–38)	450	(190–1000)	490	(300–810)
Σmono-*ortho* co-PCBs	1600	(680–3100)	4000	(730–8900)	47,000	(21,000–83,000)	96,000	(20,000–180,000)
Σco-PCBs	1600	(690–3100)	4000	(740–8900)	47,000	(22,000–84,000)	96,000	(21,000–180,000)
TEQs[a]								
ΣPCDDs-TEQs	0.015		0.015		0.30		0.30	
ΣPCDFs-TEQs	0.12	(0.055–0.25)	0.10	(0.052–0.16)	3.3	(1.6–6.6)	2.5	(1.5–3.5)
ΣPCDD/Fs TEQs	0.13	(0.070–0.27)	0.12	(0.067–0.18)	3.6	(1.9–6.9)	2.8	(1.8–3.8)
Σnon-*ortho* co-PCBs-TEQs	1.1	(0.44–2.8)	1.4	(0.74–2.8)	33	(13–76)	34	(21–59)
Σmono-*ortho* co-PCBs-TEQs	0.048	(0.020–0.092)	0.12	(0.022–0.27)	1.4	(0.63–2.5)	2.9	(0.61–5.3)
Σco-PCBs-TEQs	1.2	(0.47–2.9)	1.5	(0.76–3.0)	34	(14–78)	37	(23–63)
Σ TEQs	1.3	(0.54–3.2)	1.6	(0.90–3.2)	38	(16–85)	40	(25–66)
Other OCs[b]	concentration (ng/g wet wt)				concentration (ng/g lipid wt)			
PCBs	13	(5.5–22)	35	(5.6–93)	400	(210–660)	950	(190–1900)
DDTs	14	(4.1–31)	62	(5.7–210)	450	(160–960)	1600	(190–4300)
HCHs	24	(16–30)	28	(14–48)	750	(560–930)	790	(480–1300)
CHLs	7.4	(3.2–13)	20	(2.7–67)	240	(120–380)	540	(92–1400)
HCB	11	(6.3–15)	16	(3.5–57)	330	(190–460)	430	(120–1200)

Body length of the immature and mature minke whales used in this study was 5.8 m on average (range: 4.4–7.0 m) and 7.3 m (range: 6.9–7.7 m), respectively.
Lipid content of the liver samples of the immature and mature minke whales used in this study was 3.4 percent on average (range: 2.6–4.4 percent) and 4.0 percent (range: 3.2–5.5 percent), respectively.
For the calculation of arithmetic mean of concentrations and TEQ values, the concentrations below detection limit were regarded to be the half of the detection limit.

[a] TEQs were calculated using TEFs for mammals reported by Van den Berg et al. (2006).
[b] Data on concentrations of other OCs were cited from Niimi et al. (2005).

oceanic ecosystem. A recent report has described the hepatic TEQ levels in oceanic vertebrates (Moon et al., 2010). The hepatic TEQ levels in minke whales and common dolphins from Korean coastal waters are within the range of 4.6–66 pg TEQ/g lipid wt and 13–122 pg TEQ/g lipid wt, respectively, which are similar to those of the common minke whales from the North Pacific.

4.2. Analysis of gene expression

To investigate whether OC accumulation in the liver results in changes in the gene expression profile of the common minke whale from the North Pacific, our previous study initially examined the relationships between hepatic residue levels of OCs (PCBs, DDTs, CHLs, HCHs, and HCB) other than DRCs and the expression levels of seven CYP (*CYP*1*A*1, 1*A*2, 2*C*78, 2*E*1, 3*A*72, 4*A*35, and 4*V*6) isozymes (Niimi et al., 2007). The results indicated no clear correlation between any of the *CYPs* with a specific OC. In the present study, the relationship between DRC concentration and *CYP* levels, including that of *CYP*1*A*1 and 1*A*2, were further examined; however, no correlation was detected at any statistically significant level (data not shown). Supporting these results were the observation that the liver TEQ levels (range: 0.54–3.2 pg/g wet wt) of the common minke whales were markedly lower than the EC_{50} values for CYP1A or EROD induction by TCDD in the human hepatoblastoma cell line, HepG2 (220 pg/mL) and rat hepatoma cell line, H4IIE (16 pg/mL) (Zeiger et al., 2001). In an aquatic mammalian species, the Baikal seal (*Pusa sibirica*), the wild population had a significant positive correlation between hepatic total TEQ and CYP1A protein expression levels, showing 65 pg/g wet wt of total TEQ-EC_{50} estimated from the sigmoidal curve of the correlation (Hirakawa et al., 2007). Our recent study evaluated the sensitivity of *CYP*1*A*1 transactivation *via* AHR to TCDD in the Baikal seal by constructing an *in vitro* reporter gene assay system (Kim et al., 2011). The Baikal seal AHR (bsAHR) expression plasmid and a reporter plasmid containing *CYP*1*A*1 promoter were transfected to COS-7 cells, and the cells were treated with TCDD. The EC_{50} of TCDD was 0.021 nM (6.8 pg/mL). Comparison with the total TEQ-EC_{50} in the wild seal population and TCDD-EC_{50} for bsAHR-mediated transactivation indicates that the hepatic total TEQs in North Pacific whales were relatively low. These results thus suggest that the hepatic TEQs in this population may not reach a level that is sufficient enough to induce CYP1A. Nonetheless, a significant positive correlation ($r_s=0.64$; $p<0.01$) between *CYP*1*A*1 and *CYP*1*A*2 mRNA levels was observed (Niimi et al., 2007), which suggests that certain exogenous/endogenous AHR ligands might be regulating the expression of both *CYPs* and/or there might be a common mechanism that controls the constitutive expression of these *CYP1A* genes in the whale liver.

Apart from the correlation analysis with *CYP* expression levels, the results of the present study using a customized oligo array suggest that the hepatic expression levels of multiple genes might have been altered by the accumulation of OCs in common minke whales. Consequently, we identified 32 genes whose expression levels might have been potentially affected by DRCs and other OCs (Tables 5 and 6). Of these genes, seven (*DBP*, *ARA*70, *KYNU*, *RPS*3, *OAS*1, *LDHA*, and *CASP*6) mRNA expression levels as determined using the oligo array and real-time RT-PCR approaches showed positive correlations with any of the OC levels.

DBP mRNA expression levels measured using the real-time RT-PCR were negatively correlated ($r_s=-0.59$; $p=0.013$) with the concentrations of non-*ortho* coplanar PCB126 (Fig. 1A). DBP is a

Table 4
Results (correlation coefficients) of Pearson's correlation test between concentrations of OCs detected in the liver of common minke whales ($n=19$).

	TEQs	PCBs	DDTs	HCHs	CHLs
PCBs	0.797***				
DDTs	0.725**	0.976***			
HCHs	0.584*	0.691*	0.669*		
CHLs	0.800***	0.984***	0.970***	0.709**	
HCB	0.717**	0.714**	0.690*	0.850***	0.772**

* $p<0.01$.
** $p<0.001$.
*** $p<0.0001$.

Table 5
List of genes of which the mRNA expression levels were correlated with hepatic TEQs of PCDD/Fs and coplanar PCBs in common minke whales ($n=19$).

Gene name	Gene symbol	Compound	R^2	Slope	*p*-Value
Receptor					
Androgen receptor-associated coregulator 70; nuclear receptor coactivator 4	ARA70	Non-*ortho* co-PCBs	0.43	1.1	0.0056
Asialoglycoprotein receptor 2	ASGPR 2	PCDFs	0.37	1.0	0.013
Synthetase					
ATP synthase gamma chain	ATP5C1	Mono-*ortho* co-PCBs	0.38	−0.70	0.011
Phosphatase					
Paraoxonase 2	PON 2	Non-*ortho* co-PCBs	0.39	−1.0	0.0095
Ribosomal protein					
Ribosomal protein S3	RPS3	Non-*ortho* co-PCBs	0.48	1.3	0.0028
Ribosomal protein L13a	RPL13A	Non-*ortho* co-PCBs	0.30	1.4	0.029
Acidic ribosomal phosphoprotein P0	RPLP0	Mono-*ortho* co-PCBs	0.34	0.53	0.018
Other enzymes					
Sorbitol dehydrogenase	SORD	PCDFs	0.37	−0.76	0.013
Homogentisate 1,2-dioxygenase (Homogentisate oxidase)	HGD	Non-*ortho* co-PCBs	0.51	−1.4	0.0018
Kynureninase (L-kynurenine hydrolase)	KYNU	Non-*ortho* co-PCBs	0.33	−1.3	0.020
L-arginine:glycine amidinotransferase	LAGA	Mono-*ortho* co-PCBs	0.26	1.4	0.046
Histamine N-methyltransferase	HNMT	Mono-*ortho* co-PCBs	0.34	−3.1	0.018
Peptidylprolyl isomerase C	PPIC	Non-*ortho* co-PCBs	0.31	−2.0	0.025
N-acylsphingosine amidohydrolase (Acid ceramidase)-like (Predicted) [*Rattus norvegicus*]	ASAH1-like	Non-*ortho* co-PCBs	0.34	1.0	0.018
Others					
Vitamin D binding protein	DBP	Non-*ortho* co-PCBs	0.31	−1.3	0.025
T-cell activation protein (PGR1 protein) (Mof4 family associated protein 1)	PGR1	Non-*ortho* co-PCBs	0.27	−0.68	0.038
RER1 protein	RER1	Non-*ortho* co-PCBs	0.34	0.61	0.018
Small EDRK-rich factor 2	SERF2	Non-*ortho* co-PCBs	0.27	1.1	0.042
Plasminogen	PLG	Non-*ortho* co-PCBs	0.26	1.0	0.043
Thioredoxin domain containing 4	TXNDC4	Mono-*ortho* co-PCBs	0.36	−0.68	0.014
HSPC176 (Trafficking protein particle complex 2-like)	HSPC176	Non-*ortho* co-PCBs	0.31	1.6	0.026

Correlations were examined by stepwise multiple linear regression analysis using data on the mRNA expression levels of each gene from oligo array analyses and TEQ levels.

Table 6
List of genes of which the mRNA expression levels were correlated with hepatic concentrations of OCs other than PCDD/Fs and coplanar PCBs in common minke whales ($n=19$).

Gene name	Gene symbol	Compound	R^2	Slope	p-Value
Synthetase					
2′,5′-oligoadenylate synthetase 1	OAS1	HCB	0.33	1.3	0.019
Solute carrier family 27 (fatty acid transporter), member 5	SLC27A5	PCBs	0.53	0.85	0.0013
Enzyme					
Urate oxidase	UOX	PCBs	0.41	−0.60	0.0080
Cysteine dioxygenase type I	CDO1	HCHs	0.29	−2.0	0.032
Acetyl-Coenzyme A acetyltransferase 1	ACAT1	PCBs	0.27	−0.75	0.040
Fumarate hydratase	FH	PCBs	0.26	−0.64	0.044
Lactate dehydrogenase A	LDHA	PCBs	0.30	−0.99	0.029
Caspase 6	CASP6	PCBs	0.26	−0.44	0.044
Paraoxonase 2	PON2	HCB	0.30	−0.62	0.028
MGC					
Unknown (protein for MGC:37838)		PCBs	0.30	1.0	0.029
Others					
Annexin A5	ANXA5	HCHs	0.38	−2.3	0.011
Actin-interacting protein 1	AIP1	PCBs	0.31	0.91	0.027

Correlations were examined by stepwise multiple linear regression analysis using data on the mRNA expression levels of each gene from oligo array analyses and OC levels.

Table 7
Results of Spearman's rank correlation test between hepatic gene expression levels measured using oligo array and real-time RT-PCR analyses.

Gene symbol	r_s- Value	p-Value
ARA70	0.95	0.015
ATP5C1	0.34	0.19
PON2	0.45	0.079
RPS3	0.95	0.018
RPL13A	−0.27	0.30
RPLP0	0.23	0.37
KYNU	0.81	0.0018
HNMT	0.97	0.00020
DBP	0.39	0.13
OAS1	0.42	0.10
SLC27A5	0.18	0.49
UOX	0.27	0.31
CDO1	0.65	0.012
ACAT1	0.49	0.060
LDHA	0.80	0.0019
CASP6	0.51	0.048

See Tables 5 and 6 for the gene name of each gene symbol used in this Table.

blood transporter of vitamin D3 and its active metabolites, 25-hydroxy vitamin D3 (25-OH-D3) and 1,25-dihydroxy vitamin D3 (1α, 25-$(OH)_2$-D3), and vitamin D receptor (VDR) is activated by 1α, 25-$(OH)_2$-D3 (Safadi et al., 1999; Christakos et al., 2003; Ting et al., 2005). Considering that *DBP* mRNA levels decrease with higher dioxin-like PCB concentrations, the AHR agonist could prevent the distribution of the biologically active form of vitamin D3 through the blood stream and result in the reduction of VDR activation in peripheral tissues. Consistent with our results, Lilienthal et al. (2000) has reported that exposure to PCB mixtures, which were reconstituted based on the PCB congener profile in human breast milk, dose-dependently reduced serum concentrations of 1α, 25-$(OH)_2$-D3 in the dam and offspring of Long-Evans rats. Another study has also demonstrated that 25-(OH)-D3 levels in the plasma of Long-Evans rats decreased after TCDD treatment (Fletcher et al., 2005). In addition, 1α,25-$(OH)_2$-D3 has been associated with the anti-proliferative effects on human cancer cells through VDR (Caputo et al., 2003), as well as with the control of physiological conditions such as the immune system and calcium homeostasis (Holick, 2003). Thus, the accumulation of the coplanar PCB may lead to cancer promotion and physiological disturbances through the reduced circulation of hydroxylated vitamin D3 in minke whales. Besides, it has also been reported that the circulatory reduction of hydroxylated vitamin D3 forms could reduce *CYP2C* and *CYP3A* expression through VDR because the ligand-activated VDR regulates the expression of multiple target genes, including *CYP2C* and *CYP3A* (Pascussi et al., 2003). This earlier finding is consistent with the result of the current study in which *DBP* expression was positively correlated with both *CYP2C78* and *CYP3A72* in the liver of minke whales (Fig. 2A and B).

ARA70 mRNA levels quantified by the real-time RT-PCR analysis showed a significant positive correlation with PCB169 levels (Fig. 1C). ARA70, which is also known as nuclear receptor coactivator 4 (NCOA4), is a co-regulator of the androgen receptor (AR) and is involved in the stability of AR (Hu et al., 2004). Ting et al. (2005) suggested that AR shares ARA70 with VDR in both receptor-mediated signaling cascades, and the crosstalk between these two receptors is hence mediated by competing for ARA70. Following the increased expression of *ARA70* as induced by coplanar PCB169, the enhancement of AR-mediated signaling could induce the suppression of VDR-mediated signaling in a competitive manner, together with the decreased delivery of vitamin D as previously described.

KYNU mRNA levels and PCB126 concentrations showed a significant negative correlation (Fig. 1B). KYNU participates in the tryptophan metabolic pathway (Dale et al., 2000; Allegri et al., 2004; Stone and Darlington 2002) and plays an important role in the biosynthesis of the nicotinamide adenine dinucleotide [NAD(H)] and its phosphorylated form, NADP(H). In this pathway, KYNU catalyzes the hydrolysis of kynurenine to anthranilic acid and of 3-hydroxykynurenin to 3-hydroxyanthranilic acid (Dale et al., 2000; Allegri et al., 2004). Mostafa et al. (1983) investigated the effects of a technical PCB mixture, Aroclor 1254, on the tryptophan metabolic pathway, in which PCB-treated mice showed a reduction of KYNU and kynurenine aminotransferase activities in the liver. These observations may eventually lead to the accumulation of kynurenines, thus affecting the nervous and immune systems because kynurenines are involved in a wide range of physiological and pathological processes (Opitz et al., 2011). More recently, some investigations have revealed that kynurenine is an endogenous AHR ligand that alters the generation of regulatory T cells and IL-17-producing helper T cells (Nguyen et al., 2010; Mezrich et al., 2010).

Using data on mRNA expression levels of *RPS3*, *OAS1*, *LDHA*, and *CASP6* determined by real-time RT-PCR, an upregulation of *OAS1*, *RPS3*, *CASP6*, and *LDHA* with increasing concentrations of γ-HCH

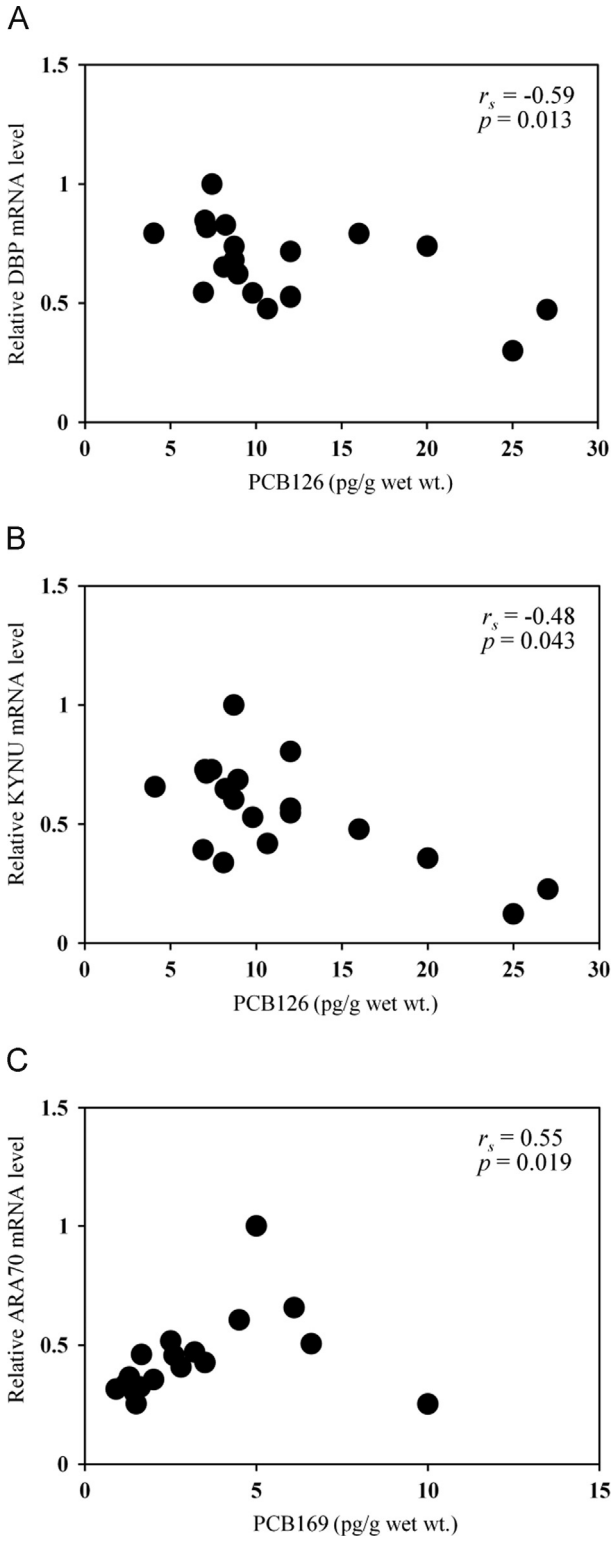

Fig. 1. Relationship between coplanar PCB concentrations and (A) *DBP*, (B) *KYNU*, or (C) *ARA70* expression levels in the liver of the common minke whale. The mRNA levels of these genes were quantified using real-time RT-PCR and expressed as the ratio relative to the highest expression level observed among all analyzed samples. The relationships were statistically examined using Spearman's rank correlation test.

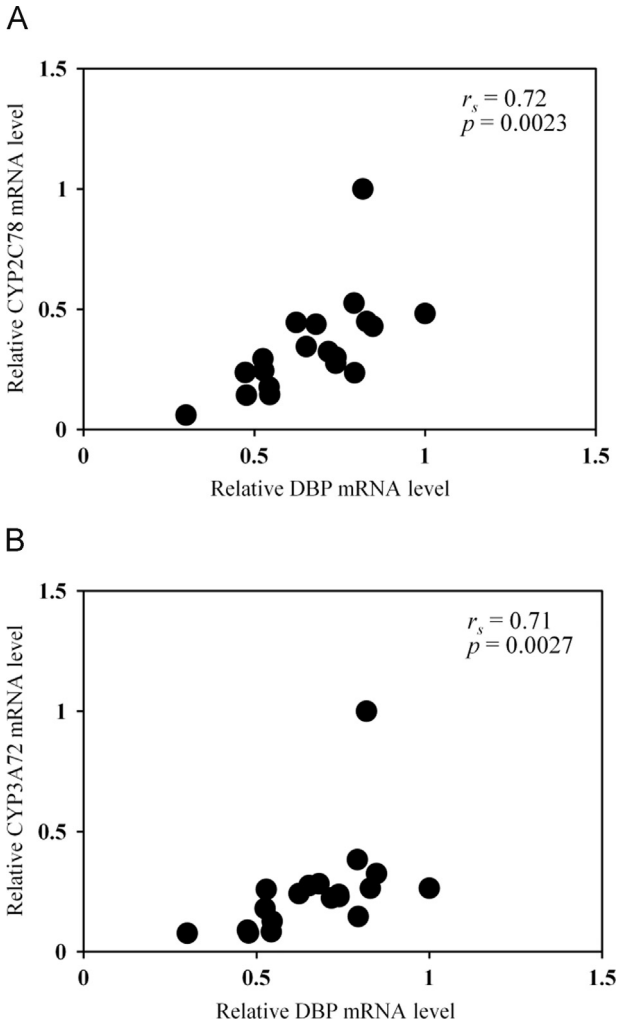

Fig. 2. Relationship between the expression level of *DBP* and (A) *CYP2C78* or (B) *CYP3A72* in the liver of common minke whales. The mRNA levels of these genes were quantified using real-time RT-PCR and expressed as the ratio relative to the highest expression level observed among all analyzed samples. The relationships were statistically examined using Spearman's rank correlation test.

was suggested (data not shown). Because these genes are associated with apoptosis (Cohen, 1997; Shim et al., 1998; Chawla-Sarkar et al., 2003; Jang et al., 2004), it is thus possible that alterations in the expression profile of the minke whale liver cells due to chemical exposure could result in apoptosis induction.

5. Conclusions

The present study indicated that hepatic expression levels of multiple genes are associated with the accumulation of OCs in the common minke whale from the North Pacific. The OC levels analyzed in this study appeared not to reach the levels that directly alter the expression of *CYP*1, 2, 3, and 4 isozymes. Nevertheless, some genes other than *CYPs* were significantly correlated with OC concentrations. This suggests that these OC concentrations may be of concern in terms of effects. We imply that exposure to coplanar PCBs resulted in a suppression of VDR-mediated signaling cascades in peripheral tissues by reducing DBP expression, and led to a downregulation of the transcription of hepatic *CYP2C* and 3*A* genes. The suppression of VDR signaling pathway might have been induced by competing with the AR-mediated signaling pathway for ARA70, which was upregulated by the accumulation of coplanar PCBs. In addition, a decrease in hepatic *KYNU* expression due to the exposure to coplanar PCBs might result in the enhanced accumulation of an endogenous aryl

hydrocarbon receptor, kynurenine, which might consequently disrupt the nervous and immune systems. On the other hand, confounding factors such as physiological parameters (age, lipid, and diet) other than chemical exposure may also be involved in altered expression levels of these genes. In conclusion, this study demonstrates that the minke whale oligo array may serve as a useful tool in screening for potential genes that could have been affected by the exposure to various environmental chemicals. Since this study does not provide physiological and biochemical validation, further research is necessary to evaluate the toxicological effects associated with the altered gene expressions.

Acknowledgments

The authors thank Prof. A. Subramanian (CMES, Ehime University) for critical reading of the manuscript. This work was supported by the Grants-in-Aid for Scientific Research (S) (21221004 and 26220103) to H.I. and (S) (20221003) to S.T., and Joint Research Project under the Japan-Korea Basic Scientific Cooperation Program for FY 2012 from the Japan Society for the Promotion of Science. Financial assistance was also provided by Global COE Program from the Ministry of Education, Culture, Sports, Science and Technology, Japan. Funding support was also given to E-Y.K. from the Basic Science Research Program through the National Research Foundation of Korea (NRF) funded by the Ministry of Education, Science and Technology, Korea (2013R1A1A2A10010043 and 2012K2A2A4021504).

References

Adeeko, A., Li, D., Doucet, J., Cooke, G.M., Trasler, J.M., Robaire, B., Hales, B.F., 2003. Gestational exposure to persistent organic pollutants: maternal liver residues, pregnancy outcome, and effects on hepatic gene expression profiles in the dam and fetus. Toxicol. Sci. 72, 242–252.

Allegri, G., Ragazzi, E., Costa, C.V., Caparrotta, L., Biasiolo, M., Comai, S., Bertazzo, A., 2004. Tryptophan metabolism along the kynurenine pathway in diet-induced and genetic hypercholesterolemic rabbits. Clin. Chim. Acta 350, 41–49.

Ankley, G.T., Bennett, R.S., Erickson, R.J., Hoff, D.J., Hornung, M.W., Johnson, R.D., Mount, D.R., Nichols, J.W., Russom, C.L., Schmieder, P.K., Serrrano, J.A., Tietge, J.E., Villeneuve, D.L., 2010. Adverse outcome pathways: a conceptual framework to support ecotoxicology research and risk assessment. Environ. Toxicol. Chem. 29 (3), 730–741.

Aono, S., Tanabe, S., Fujise, Y., Kato, H., Tatsukawa, R., 1997. Persistent organochlorines in minke whale (*Balaenoptera acutorostrata*) and their prey species from the Antarctic and the North Pacific. Environ. Pollut. 1, 81–89.

Boverhof, D.R., Burgoon, L.D., Tashiro, C., Chittim, B., Harkema, J.R., Jump, D.B., Zacharewski, T.R., 2005. Temporal and dose-dependent hepatic gene expression patterns in mice provide new insights into TCDD-mediated hepatotoxicity. Toxicol. Sci. 85, 1048–1063.

Boverhof, D.R., Burgoon, L.D., Tashiro, C., Sharratt, B., Chittim, B., Harkema, J.R., Mendrick, D.L., Zacharewski, T.R., 2006. Comparative toxicogenomic analysis of the hepatotoxic effects of TCDD in Sprague Dawley rats and C57BL/6 mice. Toxicol. Sci. 94, 398–416.

Caputo, A., Pourgholami, M.H., Akhter, J., Morris, D.L., 2003. 1,25-Dihydroxyvitamin D(3) induced cell cycle arrest in the human primary liver cancer cell line HepG2. Hepatol. Res. 26, 34–39.

Chawla-Sarkar, M., Lindner, D.J., Liu, Y.-F., Williams, B.R., Sen, G.C., Silverman, R.H., Borden, E.C., 2003. Apoptosis and interferons: role of interferon-stimulated genes as mediators of apoptosis. Apoptosis 8, 237–249.

Christakos, S., Dhawan, P., Liu, Y., Peng, X., Porta, A., 2003. New insights into the mechanisms of vitamin D action. J. Cell. Biochem. 88, 695–705.

Cohen, G.M., 1997. Caspases: the executionsers of apoptosis. Biochem. J. 326, 1–16.

Dale, W.E., Dang, Y., Brown, O.R., 2000. Tryptophan metabolism through the kynurenine pathway in rat brain and liver slices. Free Radic. Biol. Med. 29, 191–198.

Fletcher, N., Giese, N., Schmidt, C., Stern, N., Lind, P.M., Viluksela, M., Tuomisto, J.T., Tuomisto, J., Nau, H., Hakansson, H., 2005. Altered retinoid metabolism in female Long-Evans and Han/Wistar rats following long-term 2,3,7,8-tetrachlorodibenzo-*p*-dioxin (TCDD)-treatment. Toxicol. Sci. 86, 264–272.

Hirakawa, S., Iwata, S., Takeshita, Y., Kim, E.Y., Sakamoto, T., Okajima, Y., Amano, M., Miyazaki, N., Petrov, E.A., Batoev, V.B., Tanabe, S., 2007. Molecular characterization of cytochrome P4501A1, 1A2, and 1B1, and effects of polychlorinated dibenzo-*p*-dioxin, dibenzofuran, and biphenyl congeners on their hepatic expression in Baikal seal (*Pusa sibrica*). Toxicol. Sci. 97, 318–335.

Hirakawa, S., Imaeda, D., Nakayama, K., Udaka, M., Kim, E.Y., Kunisue, T., Ogawa, M., Matsuda, T., Matsui, S., Petrov, E.A., Batoev, V.B., Tanabe, S., Iwata, H., 2011. Integrative assessment of potential effects of dioxins and related compounds in wild Baikal seals (*Pusa sibirica*): application of microarray and biochemical analyses. Aquat. Toxicol. 105, 89–99.

Holick, M.F., 2003. Vitamin D: a millenium perspective. J. Cell. Biochem. 88 (2), 296–307.

Hu, Y.C., Yeh, S., Yeh, S.D., Sampson, E.R., Huang, J., Li, P., Hsu, C.L., Ting, H.J., Lin, H.K., Wang, L., Kim, E., Ni, J., Chang, C., 2004. Functional domain and motif analyses of androgen receptor coregulator ARA70 and its differential expression in prostate cancer. J. Biol. Chem. 279, 33438–33446.

Iwata, H., Tanabe, S., Sakai, N., Tatsukawa, R., 1993. Distribution of persistent organochlorines in the oceanic air and surface seawater and the role of ocean on their global transport and fate. Environ. Sci. Technol. 27 (6), 1080–1098.

Iwata, H., Watanabe, M., Okajima, Y., Tanabe, S., Amano, M., Miyazaki, N., Petrov, E. A., 2004. Toxicokinetics of PCDD, PCDF, and coplanar PCB congeners in Baikal seals, *Pusa sibirica*: age-related accumulation, maternal transfer, and hepatic sequestration. Environ. Sci. Technol. 38, 3505–3513.

Jang, C.Y., Lee, J.Y., Kim, J., 2004. RpS3, a DNA repair endonuclease and ribosomal protein, is involved in apoptosis. FEBS Lett. 56, 81–85.

Kajiwara, N., Watanabe, M., Amano, M., Yamada, T., Tanabe, S., 2004. Species-specific accumuration of dioxin related compounds in cetaceans collected from Japanease coastal waters. Organohalogen Compd. 66, 1554–1558.

Kajiwara, N., Kunisue, T., Kamikawa, S., Ochi, Y., Yano, S., Tanabe, S., 2006. Organohalogen and organotin compounds in killer whales mass-stranded in the Shiretoko Peninsula, Hokkaido, Japan. Mar. Pollut. Bull. 52, 1066–1076.

Kim, E.Y., Iwata, H., Fujise, Y., Tanabe, S., 2004. Searching for novel CYP members using cDNA library from a minke whale liver. Mar. Environ. Res. 58, 495–498.

Kim, E.Y., Suda, T., Tanabe, S., Batoev, V.B., Petrov, E.A., Iwata, H., 2011. Evaluation of relative potencies for in vitro transactivation of the Baikal Seal aryl hydrocarbon receptor by dioxin-like compounds. Environ. Sci. Technol. 45, 1652–1658.

Kopec, A.K., Burgoon, L.D., Ibrahim-Aibo, D., Burg, A.R., Lee, A.W., Tashiro, C., Potter, D., Sharratt, B., Harkema, J.R., Rowlands, J.C., Budinsky, R.A., Zacharewski, T.R., 2010. Automated dose–response analysis and comparative toxicogenomic evaluation of the hepatic effects elicited by TCDD, TCDF, and PCB126 in C57BL/6 mice. Toxicol. Sci. 118, 286–297.

Kubota, A., Watanabe, M., Kunisue, T., Kim, E.Y., Tanabe, S., Iwata, H., 2010. Hepatic CYP1A induction by chlorinated dioxins and related compounds in the endangered black-footed albatross from the North Pacific. Environ. Sci. Technol. 44, 3559–3565.

Kunisue, T., Nakanishi, S., Oka, N., Sato, F., Tsurumi, M., Tanabe, S., 2006. Dioxins and related compounds in albatrosses from the Torishima Island, Japan: accumulation features by growth stage and toxicological implications. Environ. Sci. Technol., 40; , pp. 6919–6927.

Lilienthal, H., Fastabend, A., Hany, J., Kaya, H., Roth-Harer, A., Dunemann, L., Winneke, G., 2000. Reduced levels of 1,25-dihydroxyvitamin D(3) in rat dams and offspring after exposure to a reconstituted PCB mixture. Toxicol. Sci. 57, 292–301.

Mezrich, J.D., Fechner, J.H., Zhang, X., Johnson, B.P., Burlingham, W.J., Bradfield, C.A., 2010. An interaction between kynurenine and the aryl hydrocarbon receptor can generate regulatory T cells. J. Immunol. 185, 3190–3198.

Moon, H.B., Kannan, K., Choi, H.G., An, Y.R., Choi, S.G., Park, J.Y., Kim, Z.G., 2010. Concentrations and accumulation features of PCDDs, PCDFs and dioxin-like PCBs in cetaceans from Korean coastal waters. Chemosphere 79 (9), 733–739.

Mostafa, M.H., El-Bassiouni, E.A., El-Sewedy, S.M., El-Zoghby, S.M., Ramadan, M., Abdel-Tawab, G.A., El-Sebae, A.H., 1983. Effect of some xenobiotics on kynurenine hydrolase and kynurenine aminotransferase of mouse liver. J. Environ. Sci. Health B 18, 393–399.

Nakayama, K., Iwata, H., Kim, E.Y., Tashiro, K., Tanabe, S., 2006. Gene expression profiling in common cormorant liver with an oligo array: assessing the potential toxic effects of environmental contaminants. Environ. Sci. Technol. 40, 1076–1083.

Nguyen, N.T., Kimura, A., Nakahama, T., Chinen, I., Masuda, K., Nohara, K., Fujii-Kuriyama, Y., Kishimoto, T., 2010. Aryl hydrocarbon receptor negatively regulates dendritic cell immunogenicity via a kynurenine-dependent mechanism. Proc. Natl. Acad. Sci. USA 107, 19961–19966.

Niimi, S., Watanabe, M.X., Kim, E.Y., Iwata, H., Yasunaga, G., Fujise, Y., Tanabe, S., 2005. Molecular cloning and mRNA expression of cytochrome P4501A1 and 1A2 in the liver of common minke whales (*Balaenoptera acutorostrata*). Mar. Pollut. Bull. 51, 784–793.

Niimi, S., Kim, E.Y., Iwata, H., Watanabe, M.X., Yasunaga, G., Fujise, Y., Tanabe, S., 2007. Identification and hepatic expression profiles of cytochrome P450 1-4 isozymes in common minke whales (*Balaenoptera acutorostrata*). Comp. Biochem. Physiol. B Biochem. Mol. Biol. 147, 667–681.

Opitz, C.A., Litzenburger, U.M., Sahm, F., Ott, M., Tritschler, I., Trump, S., Schumacher, T., Jestaedt, L., Schrenk, D., Weller, M., Jugold, M., Guillemin, G.J., Miller, C. L., Lutz, C., Radlwimmer, B., Lehmann, I., von Deimling, A., Wick, W., Platten, M., 2011. An endogenous tumour-promoting ligand of the human aryl hydrocarbon receptor. Nature 478 (7368), 197–203.

Pascussi, J.M., Gerbal-Chaloin, S., Drocourt, L., Maurel, P., Vilarem, M.J., 2003. The expression of CYP2B6, CYP2C9 and CYP3A4 genes: a tangle of networks of nuclear and steroid receptors. Biochim. Biophys. Acta 1619, 243–253.

Safadi, F.F., Thornton, P., Magiera, H., Hollis, B.W., Gentile, M., Haddad, J.G., Liebhaber, S.A., Cooke, N.E., 1999. Osteopathy and resistance to vitamin D toxicity in mice null for vitamin D binding protein. J. Clin. Investig. 103, 239–251.

Shim, H., Chun, Y.S., Lewis, B.C., Dang, C.V., 1998. A unique glucose-dependent apoptotic pathway induced by c-Myc. Proc. Natl. Acad. Sci. USA 95, 1511–1516.
Stone, T.W., Darlington, L.G., 2002. Endogenous kynurenines as targets for drug discovery and development. Nat. Rev. Drug Discov. 1 (8), 609–620.
Tamura, T., Fujise, Y., 2002. Geographical and seasonal changes of the prey species of minke whale in the Northwestern Pacific. J. Mar. Sci. 59, 516–528.
Tanabe, S., Iwata, H., Tatsukawa, R., 1994. Global contamination by persistent organochlorines and their ecotoxicological impact on marine mammals. Sci. Total Environ. 154, 163–177.
Ting, H.J., Bao, B.Y., Hsu, C.L., Lee, Y.F., 2005. Androgen-receptor coregulators mediate the suppressive effect of androgen signals on vitamin D receptor activity. Endocrine 26 (1), 1–9.
Van Aggelen, G., Ankley, G.T., Baldwin, W.S., Bearden, D.W., Benson, W.H., Chipman, J.K., Collette, T.W., Craft, J.A., Denslow, N.D., Embry, M.R., Falciani, F., George, S. G., Helbing, C.C., Hoekstra, P.F., Iguchi, T., Kagami, Y., Katsiadaki, I., Kille, P., Liu, L., Lord, P.G., McIntyre, T., O'Neill, A., Osachoff, H., Perkins, E.J., Santos, E.M., Skirrow, R.C., Snape, J.R., Tyler, C.R., Versteeg, D., Viant, M.R., Volz, D.C., Williams, T.D., Yu, L., 2010. Integrating omic technologies into aquatic ecological risk assessment and environmental monitoring: hurdles, achievements, and future outlook. Environ. Health Perspect. 118, 1–5.
Van den Berg, M., Birnbaum, L.S., Denison, M., De Vito, M., Farland, W., Feeley, M., Fiedler, H., Hakansson, H., Hanberg, A., Haws, L., Rose, M., Safe, S., Schrenk, D., Tohyama, C., Tritscher, A., Tuomisto, J., Tysklind, M., Walker, N., Peterson, R.E., 2006. The 2005 World Health Organization re-evaluation of human and mammalian toxic equivalency factors for dioxins and dioxin-like compounds. Toxicol. Sci. 93, 223–241.
Vezina, C.M., Walker, N.J., Olson, J.R., 2004. Subchronic exposure of TCDD, PeCDF, PCB126, and PCB153: effect on hepatic gene expression. Environ. Health Perspect. 112, 1636–1644.
Villeneuve, D.L., Garcia-Reyero, N., 2011. Vision & strategy: predictive ecotoxicology in the 21st century. Environ. Toxicol. Chem. 30 (1), 1–8.
Williams, T.D., Gensberg, K., Minchin, S.D., Chipman, J.K., 2003. A DNA expression array to detect toxic stress response in European flounder (*Platichthys flesus*). Aquat. Toxicol. 65, 141–157.
Zeiger, M., Haag, R., Hockel, J., Schrenk, D., Schmitz, H.J., 2001. Inducing effects of dioxin-like polychlorinated biphenyls on CYP1A in the human hepatoblastoma cell line HepG2, the rat hepatoma cell line H4IIE, and rat primary hepatocytes: comparison of relative potencies. Toxicol. Sci. 63, 65–73.
Zeytun, A., McKallip, R.J., Fisher, M., Camacho, I., Nagarkatti, M., Nagarkatti, P.S., 2002. Analysis of 2,3,7,8-tetrachlorodibenzo-*p*-dioxin-induced gene expression profile *in vivo* using pathway-specific cDNA arrays. Toxicology 178, 241–260.